Contribution from the W. R. Kenan, Jr., Research Laboratories, Department of Chemistry, The University of North Carolina, Chapel Hill, North Carolina 27514

Intervalence Transfer in Ligand-Bridged, Trimeric Complexes of Ruthenium

M. J. POWERS, R. W. CALLAHAN, DENNIS J. SALMON, and THOMAS J. MEYER*

Received August 15, 1975 AIC50612M

A series of ligand-bridged, trimeric complexes $[(NH_3)_5Ru(L)Ru(bpy)_2(L)Ru(NH_3)_5]^{6+}$ [2,2,2] (bpy is 2,2'-bipyridine; L is a dibasic N-heterocyclic ligand like pyrazine) and their redox properties were studied chemically and electrochemically. In the mixed-valence 8+ [3,2,3] ions the sites of oxidation are localized on the pentaammine ends which is predicted given the differences in reduction potentials for related Ru(III)–Ru(II) couples. IT (intervalence transfer) bands appear for the mixed-valence ions and the properties of the bands are discussed in terms of the Hush treatment for intervalence transfer. Spectrophotometric titrations with Br_2 in the IT spectral region show that the IT bands for the singly and twice oxidized ions [2,2,3] and [3,2,3] are similar in energy and intensity, and no evidence has been obtained for long-range interactions between the remote pentaammine groups.

Introduction

Recent studies on discrete mixed-valence compounds[1] have been based mainly on spin-paired d^5–d^6 systems including ferrocene–ferricenium derivatives and Ru(II)–Ru(III) complexes. Coordination complexes of ruthenium are very attractive for mixed-valence studies because the +2 and +3 oxidation states are accessible, complexes in either oxidation state are usually substitution inert,[2] and general synthetic routes are available for the preparation of systems in which two or more metal centers are linked by bridging ligands.[3-6]

Most of the mixed-valence work has been carried out on dimeric systems although a recent paper on mixed-valence polyferrocene ions has appeared.[7] In particular, the Creutz and Taube ion

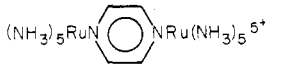

has been studied in detail.[3,4,8-12] For that ion and for related symmetrical[13]

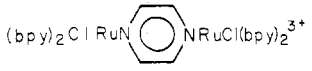

and unsymmetrical[6]

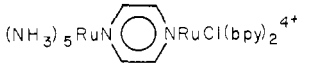

mixed-valence ions, low-energy electronic bands have been found. Unusual absorption bands often appear in mixed-valence compounds, and from their properties useful information can often be obtained concerning delocalization in the ground state.[1,14] For cases where there are discrete valences and where delocalization between the metal sites is not extensive, Hush has assigned the low-energy bands to intervalence transfer (IT) transitions where light-induced electron transfer occurs between different valence state sites.[14] Given the discrepancies in the properties of IT bands between closely related Ru systems,[3,13] it is of considerable interest to determine the applicability and limitations of the treatment given by Hush for IT bands.[14] In addition, we have a continuing interest in mixed-valence systems where there is a possibility for interactions involving more than two metal sites.[7,15-16] We report here the preparation and properties of a series of trimeric ruthenium(II) complexes in which the bridging ligands are pyrazine (pyr), 4,4'-bipyridine (4,4'-bpy), *trans*-1,2-bis(4-pyridyl)ethylene (BPE), and 1,2-bis(4-pyridyl)ethane (BPA), the conversion of the complexes to their mixed-valence forms, and an analysis of the IT bands which appear for the mixed-valence ions.

Experimental Section

Measurements. Ultraviolet, visible, and very near-infrared spectra were recorded using Cary Models 14 and 17 and Bausch and Lomb

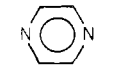

pyr

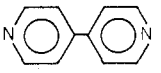

4,4'-bpy

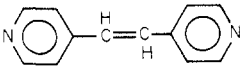

BPE

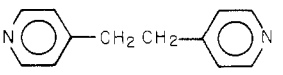

BPA

Model 210 spectrophotometers. Electrochemical measurements made were vs. the saturated sodium chloride calomel electrode (SSCE) at 25 ± 2 °C and are uncorrected for junction potential effects. The measurements were made using a PAR Model 173 potentiostat for potential control with a PAR Model 175 Universal Programmer as a sweep generator for voltammetric experiments. Values of n, where n is the total number of electrons transferred in exhaustive electrolysis at constant potential, were calculated after measuring the total area under current vs. time curves for the complete reaction. Reactions were judged to be complete when the current had fallen below 1% of its initial value. Electrochemical reversibility was determined by cyclic voltammetry, based on the ratio of cathodic to anodic peak currents (i_c/i_a) and the potential separation of the peaks (ΔE_p). All voltammetric measurements were carried out at platinum electrodes in solutions deaerated by a stream of dry argon or nitrogen.

Materials. Tetra-*n*-butylammonium hexafluorophosphate (TBAH) was prepared by standard techniques,[17] recrystallized three times from hot ethanol–water mixtures, and vacuum dried at 70 °C for 10 h. Acetonitrile (MCB Spectrograde) was dried over Davison 4-Å molecular sieves for electrochemical measurements and used without drying for spectral measurements. Water was deionized and then distilled from alkaline permanganate. All other solvents (reagent grade) were used without further purification. The ligands pyrazine (pyr), 4,4'-bipyridine (4,4'-bpy), *trans*-1,2-bis(4-pyridyl)ethylene (BPE), and 1,2-bis(4-pyridyl)ethane (BPA) were obtained commercially and used without further purification. Argon was scrubbed by passing it through a heated column of activated Catalyst R3-11 (Chemical Dynamics Corp.) and then through drying tubes containing Drierite. Elemental analyses were carried out by Galbraith Laboratories, Knoxville, Tenn.

Preparations. $[Ru(NH_3)_5Cl]Cl_2$. The salt was prepared according to the procedure of Vogt et al.[18] and recrystallized from hot (ca. 80–90 °C) 0.1 M hydrochloric acid.

$[Ru(NH_3)_5(H_2O)](PF_6)_2 \cdot H_2O$. The $[Ru(NH_3)_5H_2O]^{2+}$ ion was generated essentially as described by Harrison et al.[19] and in previous papers.[6]

$[Ru(bpy)_2(L)_2](PF_6)_2 \cdot nH_2O$ (L = pyr, 4,4'-bpy, BPE, BPA). The preparation of $[Ru(bpy)_2(pyr)_2](PF_6)_2$ has been described previously.[5,20] The salts $[Ru(bpy)_2(L)_2](PF_6)_2$, where L is 4,4'-bpy, BPE, or BPA, were prepared by similar methods. For the complexes in which L is BPE or BPA, however, the aqueous solution of the complex, after excess ligand had been removed by filtration, was adjusted to pH 7 with NaOH solutions. After neutralization a saturated solution of ammonium hexafluorophosphate, also adjusted to pH 7, was added, precipitating the hexafluorophosphate salts. Anal. Calcd for $[Ru(bpy)_2(4,4'\text{-bpy})_2](PF_6)_2$: C, 47.30; H, 3.18; N, 11.03. Found: C, 47.39; H, 3.14; N, 11.09. Calcd for $[Ru(bpy)_2(BPE)_2](PF_6)_2 \cdot 2H_2O$: C, 47.88; H, 3.65; N, 10.15. Found: C, 47.64; H, 3.42; N, 10.11. Calcd for $[Ru(bpy)_2(BPA)_2](PF_6)_2$: C, 49.31; H, 3.76; N,

10.45. Found: C, 49.17; H, 3.74; N, 10.05.

$[[Ru(NH_3)_5(L)]_2Ru(bpy)_2](PF_6)_6 \cdot nH_2O$ (L = pyr, 4,4'-bpy, BPE, BPA). In a typical preparation $[(bpy)_2Ru(4,4'\text{-}bpy)_2](PF_6)_2$ (0.236 g, 0.130 mmol) and $[Ru(NH_3)_5(H_2O)](PF_6)_2$ (0.131 g, 0.264 mmol) were deaerated with argon in a sealed Erlenmeyer flask. The flask was covered with aluminum foil to protect it from light. Deaerated acetone (20 ml) was added, and the solution stirred under argon for at least 4 h. The acetone solution was then added dropwise to 200 ml of methylene chloride, in the dark, and the precipitate collected on a glass frit. The trimeric complex was dissolved in acetone and reprecipitated by adding to ether; yield 82%. Anal. Calcd for $[[Ru(NH_3)_5(pyr)]_2Ru(bpy)_2](PF_6)_6 \cdot 2H_2O$: C, 18.16; H, 3.13; N, 13.62; F, 36.94. Found: C, 18.09; H, 3.01; N, 13.22; F, 35.30. Calcd for $[[Ru(NH_3)_5(4,4'\text{-}bpy)]_2Ru(bpy)_2](PF_6)_6$: C, 24.41; H, 3.18; N, 12.81. Found: C, 24.24; H, 3.30; N, 12.71. Calcd for $[[Ru(NH_3)_5(BPE)]_2Ru(bpy)_2](PF_6)_6$: C, 26.13; H, 3.29; N, 12.47. Found: C, 26.16;, H, 3.14; N, 11.37. Calcd for $[[Ru(NH_3)_5(BPA)]_2Ru(bpy)_2](PF_6)_6$: C, 26.11; H, 3.49; N, 12.55. Found: C, 26.82; H, 3.36; N, 11.91.

$[[Ru(NH_3)_5(L)]_2Ru(bpy)_2](PF_6)_8$ (L = pyr, 4,4'-bpy, BPE, BPA). The trimeric complex $[[Ru(NH_3)_5(pyr)]_2Ru(bpy)_2](PF_6)_6 \cdot 2H_2O$ (0.355 g, 0.192 mmol) and an excess of tetra-*n*-butylammonium hexfluorophosphate were dissolved in acetonitrile which had been deaerated by argon in a sealed Erlenmeyer flask in the dark. A 10% molar excess of Br_2 in acetonitrile was added with a syringe with stirring. The oxidation reaction is very rapid. The oxidized form of the trimer was added dropwise to 200 ml of ether and the brown precipitate collected on a glass frit, washed with methylene chloride, and reprecipitated from acetone by adding to ether. The pyrazine-bridged trimer was isolated as a solid using this procedure. The oxidized forms of the remaining trimers were generated in solution using Br_2 and were not isolated. Anal. Calcd for $[[Ru(NH_3)_5(pyr)]_2Ru(bpy)_2](PF_6)_8$: C, 15.97; H, 2.59; N, 11.97; F, 43.31. Found: C, 15.89; H, 2.62; N, 12.09; F, 43.19.

Spectrophotometric Titrations. Solutions of Br_2 in CH_3CN were standardized using ϵ 183 ± 4 M^{-1} cm^{-1} at 392 nm.[6b] All spectrophotometric titrations were carried out by adding aliquots of oxidant to solutions of the complex. The titrations were carried out in the dark in deaerated solvents and followed by monitoring the changes in absorbance at various wavelengths. To establish reaction stoichiometries, Job plots were made of absorbance at a particular wavelength (normally at an absorption maximum) vs. the ratio of moles of oxidant added to moles of complex.

Results

Ultraviolet–Visible Spectra. The important features of the spectra of the 6+ and mixed-valence 8+ trimeric ions $[[Ru(NH_3)_5(L)]_2Ru(bipy)_2]^{8+}$ and $[[Ru(NH_3)_5(L)]_2Ru(bpy)_2]^{6+}$ are given in summary form in Table I, as well as data for the related, monomeric complexes $[Ru(bpy)_2(L)_2]^{2+}$. The ultraviolet–visible spectra of pentaammine–pyridine type complexes of ruthenium in the same medium have been reported elsewhere.[6b] It should be noted that intense bands in the visible region both for pentaammine–pyridine type complexes and for bis(2,2'-bipyridine)ruthenium(II) complexes have been assigned to $d\pi$(metal) → π^*(ligand) charge-transfer (CT) absorptions.[21-23] Intense bands in the ultraviolet region have been assigned to ligand-centered $\pi \rightarrow \pi^*$ transitions.

Electrochemistry. Voltammetric half-wave potentials vs. the saturated sodium chloride calomel electrode are given in Table II for the monomeric and trimeric complexes reported here. Electrochemical results for the monomeric couples $[Ru(NH_3)_5(L)]^{3+}$–$[Ru(NH_3)_5(L)]^{2+}$ have been reported elsewhere.[6b] The potentials are formally reduction potentials (Ru(III) + e^- → Ru(II)) except for a usually small correction term involving diffusion coefficients.

A cyclic voltammogram for the [2,2,2] ions where L is pyrazine in 0.1 M $[N(n\text{-}C_4H_9)_4][PF_6]$–acetonitrile is shown in Figure 1. There are two anodic waves in the region 0–1.5 V which are labeled $E_{1/2}(1)$ and $E_{1/2}(2)$ in Table II according to their order of appearance in sweeping from 0 to 1.5 V. For the L = pyrazine case the voltammogram is consistent with two closely spaced one-electron waves for the oxidation of the

Table I. Spectral Data for Monomeric and Trimeric Complexes in Acetonitrile[a]

Complex	λ_{max},[b] nm	ϵ_{max},[c] M^{-1} cm^{-1}
$[Ru(bpy)_2(pyr)_2]^{2+}$	425 sh	
	407	1.26×10^4
	375	1.23×10^4
	345 sh	
	287	4.98×10^4
	255	2.90×10^4
	245 sh	
$[Ru(bpy)_2(4,4'\text{-}bpy)_2]^{2+}$	445 sh	
	425	6.84×10^3
	367	8.68×10^3
	290	2.69×10^4
	255 sh	
	245	2.40×10^4
$[Ru(bpy)_2(BPE)_2]^{2+}$	455 sh	
	430 sh	(2.13×10^4)
	395	2.42×10^4
	305 sh	
	292	10.38×10^4
	258	2.92×10^4
$[Ru(bpy)_2(BPA)_2]^{2+}$	448	8.18×10^3
	430 sh	
	335	1.41×10^4
	288	2.14×10^4
	243	1.02×10^3
$[[(NH_3)_5Ru(L)]_2Ru(bpy)_2]^{6+}$		
L = pyr	535	4.2×10^4
	390 sh	
	365	0.81×10^4
	288	3.64×10^4
	254	2.53×10^4
	245 sh	
L = 4,4'-bpy	522	3.41×10^4
	465 sh	
	375 sh	
	290	5.75×10^4
	254 sh	
	244	5.20×10^4
L = BPE	544	3.55×10^4
	473	(2.84)
	433 sh	
	379 sh	
	290	9.64×10^4
	256 sh	
L = BPA	465 sh	
	420	2.05×10^4
	344	2.17×10^4
	290	5.81×10^4
	244	3.46×10^4
$[[(NH_3)_5Ru(L)]_2Ru(bpy)_2]^{8+}$		
L = pyr	439	1.75×10^4
	405 sh	
	280	3.68×10^4
	252	2.12×10^4
	246 sh	
L = 4,4'-bpy	445 sh	
	428	2.30×10^4
	375 sh	
	290	7.14×10^4
	254 sh	
	244	5.14×10^4
L = BPE	450 sh	
	433	3.19×10^4
	380 sh	
	350 sh	
	312	
	291	10.2×10^4
	257	
L = BPA	456	9.64×10^3
	432 sh	
	342	1.90×10^4
	290	5.92×10^4
	245	3.72×10^4

[a] Spectra were obtained at room temperature on solutions which had been protected from ambient light. [b] ±1 nm. [c] ±5%.

Table II. Electrochemical Data[a]

Complex	$E_{1/2}(1)$, V	$E_{1/2}(2)$, V	$E_{1/2}'$, V
$[Ru(bpy)_2(pyr)_2]^{2+}$			1.51
$[Ru(bpy)_2(4,4'\text{-bpy})_2]^{2+}$			1.32
$[Ru(bpy)_2(BPE)_2]^{2+}$			1.31
$[Ru(bpy)_2(BPA)_2]^{2+}$			1.29
$[[(NH_3)_5Ru(L)]_2Ru(bpy)_2]^{6+}$			
L = pyr	0.70	1.79	
L = 4,4'-bpy	0.43	1.37	
L = BPE	0.40	1.32	
L = BPA	0.36	1.27	

[a] At a Pt bead electrode in 0.1 M $[N(n\text{-}C_4H_9)_4][PF_6]$-$CH_3CN$ vs. SSCE at 25 ± 2 °C.

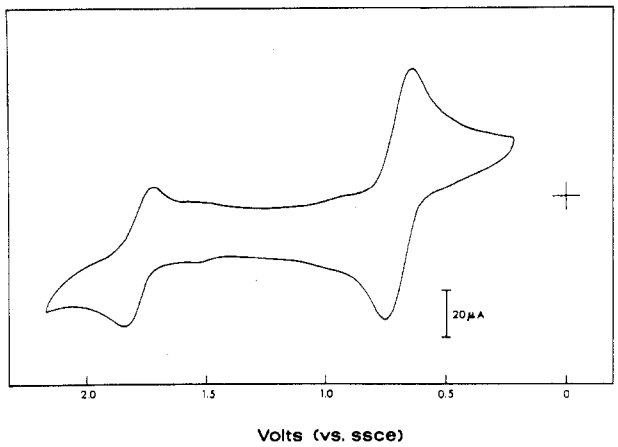

Figure 1. The 200-mV/s cyclic voltammogram of $[[(NH_3)_5Ru(pyr)]_2Ru(bpy)_2](PF_6)_6 \cdot 2H_2O$ in 0.1 M TBAH–CH_3CN.

pentaammine groups at low potential followed by oxidation of the central 2,2'-bpy group at $E_{1/2}(2)$. Coulometry on the diffusion plateau of the first wave gave n = 1.91 consistent with a two-electron oxidation. $\Delta E_p = E_{p,a} - E_{p,c}$ was independent of sweep rate for the second wave ($E_{1/2}(2)$) in all cases and for the first wave for the L = pyrazine case. For the second wave ΔE_p was slightly greater than the expected value (60–75 mV vs. 59 mV) because of uncompensated solution resistance.

For the [2,2,2] ions where L is 4,4'-bpy, BPE, or BPA, ΔE_p and i_p are dependent upon sweep rate, the peak current for the first wave is considerably less than about twice i_p for the second wave, which would have been expected, and coulometry gave values for n in the range 0.99–1.48. The origin of these effects is not clear but may be related to surface adsorption since the results obtained appeared to be sensitive to the history of the platinum electrode used.[24] Further evidence implicating surface effects is that the chemical oxidations with Br_2 are well-defined in acetonitrile, and that the electrochemistry is well-defined in aqueous solution. The first wave for the [2,2,2] ion when L = 4,4'-bpy in 0.5 M NaCl–H_2O showed that $i_{p,a}/i_{p,c} \approx 1.0$, that ΔE_p which is ~80 mV is independent of sweep rate, and that electrochemical oxidation on the diffusion plateau of the wave is consistent with a two-electron process (n = 1.98).

Spectrophotometric Titrations. The stoichiometries of the reactions between the [2,2,2] ions and bromine in acetonitrile were determined by spectrophotometric titrations. The results of a typical experiment are shown in Figure 2 for L = BPE. From the titrations the ratio of moles of Br_2 consumed to moles of trimer consumed was determined. The results were 0.98 for L = pyr, 1.15 for L = 4,4'-bpy, 0.95 for L = BPE, and 0.93 for L = BPA. The results of the titrations show that the stoichiometry is

$$[[(NH_3)_5Ru(L)]_2Ru(bpy)_2]^{6+} + Br_2 \rightarrow [[(NH_3)_5Ru(L)]_2Ru(bpy)_2]^{8+} + 2Br^- \quad (1)$$

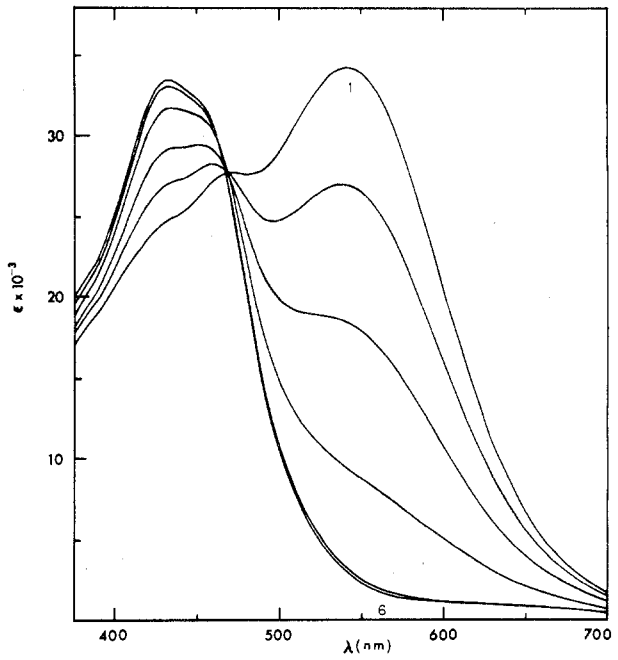

Figure 2. Visible spectrophotometric titration of $[[(NH_3)_5Ru(BPE)]_2Ru(bpy)_2]^{6+}$ by Br_2 in CH_3CN. Br_2:$[[(NH_3)_5Ru(BPE)]_2Ru(bpy)_2]^{6+}$ ratios: solution 1, 0.00; solution 2, 0.25; solution 3, 0.50; solution 4, 0.75; solution 5, 1.00; solution 6, 1.25.

Table III. Low-Energy Electronic Bands

Ion $[[(NH_3)_5Ru\text{-}(L)]_2Ru(bpy)_2]^{8+}$	λ_{max}, nm (ϵ)[a]		
	Acetonitrile	Propylene carbonate	Nitrobenzene
L = pyr	730 (900)	725 (909)	795 (1060)
L = 4,4'-bpy	605 (884)[b]		650
L = BPE			665 (1150)[b]

[a] ±5 nm; ϵ values are ±5%. [b] Because of strong overlap with tailing CT bands, these values are *not* reasonable approximations of true band intensities.

The stoichiometry is expected since Br_2 in acetonitrile rapidly oxidizes monomeric pentaammineruthenium(II) complexes, e.g., $[Ru(NH_3)_5(py)]^{2+}$, but is not a sufficiently strong oxidant to oxidize bis(2,2'-bipyridine)ruthenium(II) complexes like $[Ru(bpy)_2(py)_2]^{2+}$.

The mixed-valence 8+ ions are reduced to the 6+ ions by both hydrazine and stannous chloride in acetonitrile solution. However, in some cases the changes in absorption spectra were consistent with as little as 80% recovery of the reduced ions when hydrazine is used. The origin of the incomplete recovery appears to be a competitive reaction which is currently under investigation. It should be noted that the mixed-valence ions are stable in solution for extended periods (see below).

Spectrophotometric titrations with Br_2 were also followed in the near infrared region (600–900 nm). The results obtained for the [2,2,2] ion when L = pyr are shown in Figure 3.

Low-Energy Electronic Bands. The mixed-valence ions $[[Ru(NH_3)_5(L)]_2Ru(bpy)_2]^{8+}$, L = pyr, 4,4'-bpy, BPE, have low-energy absorption bands. Where available, data for these bands are given in some solvents in Table III. Solubility problems prevented our obtaining complete data in several cases.

The corresponding 6+ ions $[[(NH_3)_5Ru(L)]_2Ru(bpy)_2]^{6+}$ have residual light absorption in the near-infrared region because of long-wavelength tailing of broad CT bands centered in the visible region but have no distinct bands in this region. Tailing of intense visible absorption bands is also observed for the 8+ ions. In fact, for the BPE-bridged timer, a distinct

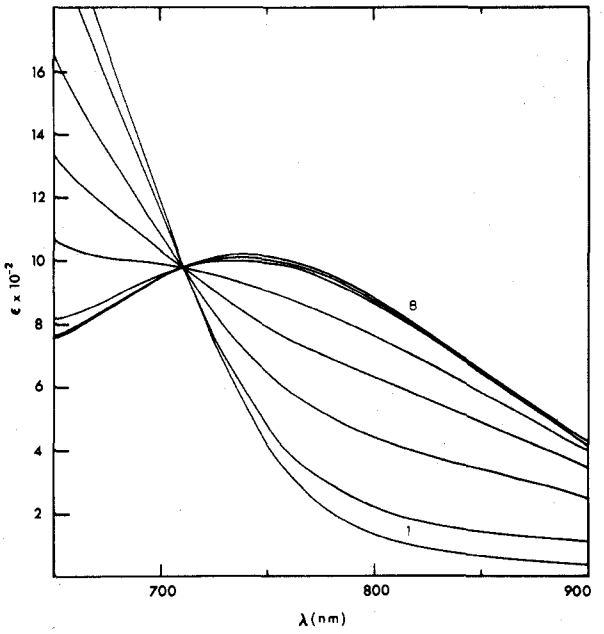

Figure 3. Near-infrared spectrophotometric titration of $[((NH_3)_5Ru(pyr))_2Ru(bpy)_2]^{6+}$ by Br_2 in CH_3CN. Br_2:$[[(NH_3)_5Ru(pyr)]_2Ru(bpy)_2]^{6+}$ ratios: solution 1, 0.00; solution 2, 0.17; solution 3, 0.33; solution 4, 0.50; solution 5, 0.67; solution 6, 0.83; solution 7, 1.00; solution 8, 1.17.

near-infrared band was observed in nitrobenzene but was not observed in either acetonitrile or propylene carbonate. In the latter two solvents the near-infrared band is apparently masked by the tailing of the intense visible CT band.

Stability of the Complexes. In the absence of light in deaerated solvents such as acetonitrile, acetone, or water, the [2,2,2] ions are stable for at least 2–3 days. The complexes undergo relatively efficient light-catalyzed decomposition reactions. When exposed to room lighting the absorbance at λ_{max} 523 nm for the 4,4'-bpy-bridged complex decreases ~10% in 15 min, in deaerated acetonitrile. After 5–6 h, the decomposition is complete. From the absorption spectra of acetonitrile solutions after prolonged exposure to light, the decomposition reactions (in the absence of oxygen) appear to involve a series of net photosolvation steps giving $[Ru(NH_3)_5(CH_3CN)]^{2+}$ and $[Ru(bpy)_2(CH_3CN)_2]^{2+}$. The 8+, mixed-valence ions are reasonably stable in deaerated acetonitrile solutions in the absence of light. Only slight changes (~10% decrease in absorption at λ_{max} 445 nm for the 4,4'-bpy-bridged trimer) were observed after 2–3 days.

The complexes are unstable in the solid state as PF_6^- salts and were stored under argon or in vacuum desiccators at 4 °C. The nature of the solid-state decomposition reaction is unknown.

Discussion

Site of Oxidation. The first oxidation of the 6+ trimers is localized largely on the pentaammine groups (eq 2). The

$$[[(NH_3)_5Ru^{II}(L)]_2Ru^{II}(bpy)_2]^{6+} \xrightarrow{-2e^-} [[(NH_3)_5Ru^{III}(L)]_2Ru^{II}(bpy)_2]^{8+} \quad (2)$$

evidence having a bearing on this conclusion includes the following. (1) The stoichiometries of the reactions of the 6+ ions with Br_2 were 1:1 (eq 1). (2) In the titrations, as oxidation proceeds, bands disappear which can be assigned to $d\pi$-$[Ru^{II}(NH_3)_5(L)] \rightarrow \pi^*(L)$ transitions (Figure 2). This is most apparent in the BPA trimer, $[[(NH_3)_5Ru(BPA)]_2Ru(bpy)_2]^{6+}$, where the absorption bands for the separate CT transitions for the $[Ru^{II}(NH_3)_5(L-)]$ and $[Ru^{II}(bpy)_2(L-)_2]$ groups are essentially unchanged from related monomeric complexes (Table I and ref 6). It should be noted that complexes of the type $[Ru^{III}(NH_3)_5(L)]^{3+}$ are relatively transparent above 400 nm. (3) The electrochemical experiments on the trimers give two $E_{1/2}$ values in acetonitrile which fall in potential ranges found for the related monomeric couples $[Ru(NH_3)_5(L)]^{3+}$–$[Ru(NH_3)_5(L)]^{2+}$ and $[Ru(bpy)_2(L)_2]^{3+}$–$[Ru(bpy)_2(L)_2]^{2+}$ (Table II and ref 6).

Ultraviolet–Visible Spectra. For the BPA trimers, $[[Ru(NH_3)_5(BPA)]_2Ru(bpy)_2]^{n+}$ (n = 6 or 8), the $Ru(NH_3)_5(L-)$ and $Ru(bpy)_2(L-)_2$ groups can be treated as separate chromophores with no evidence for metal–metal interactions across the saturated $-CH_2-CH_2-$ linkage. The observed spectra are simply the sums of spectra for the monomeric ions $[Ru(NH_3)_5(BPA)]^{2+}$ and $[Ru(NH_3)_5(BPA)]^{3+}$ [6] and $[Ru(bpy)_2(BPA)_2]^{2+}$.

For the remaining trimers where the bridging ligand includes an intact π system (pyr, 4,4'-bpy, BPE), the spectra are significantly different from simple monomeric spectra. The arguments developed in a previous paper for the spectra of the dimeric complexes $[(NH_3)_5Ru(L)RuCl(bpy)_2]^{3+}$ based on the effects of adjacent metal centers on the expected $\pi \rightarrow \pi^*(bpy)$, $\pi \rightarrow \pi^*(L)$, $d\pi[Ru^{II}(NH_3)_5(L-)] \rightarrow \pi^*(L)$, $d\pi[Ru^{II}(bpy)_2(L-)] \rightarrow \pi^*(bpy)$, and $d\pi[Ru^{II}(bpy)_2(L-)] \rightarrow \pi^*(L)$ transitions are mainly appropriate here. However, there are certain special features in the trimeric ions including unusual intensity enhancements and shifts in absorption bands which will be discussed in a later paper in conjunction with the spectra of the polymeric ions $[(bpy)_2ClRu(L)[Ru(bpy)_2(L)]_nRuCl(bpy)_2]^{(2n+2)+}$.[5]

Reduction Potentials. The reduction potentials obtained from the two oxidation waves for the trimers fall in the ranges expected for related monomeric and dimeric couples. $E_{1/2}(1)$ refers to oxidation of the pentaammine groups and $E_{1/2}(2)$ to oxidation of the central $Ru^{II}(bpy)_2(L-)_2$ groups (Table II and ref 6). The $E_{1/2}(1)$ wave is really a composite wave consisting of two one-electron processes as shown by eq 3 and 4. For the half-reactions there is a statistical factor of $^1/_2$

$$[2,2,3] + e^- \rightarrow [2,2,2] \quad (3)$$

$$[3,2,3] + e^- \rightarrow [2,2,3] \quad (4)$$

for eq 3 and of 2 for eq 4, as written.[25,26] The statistical factor leads to a potential difference for the two waves which can be calculated as (RT/nF) ln 4 = 0.036 V. Electrostatic effects will increase the potential difference slightly, if at all, and differential delocalization in the mixed-valence [2,2,3] and [3,2,3] ions is probably small (see below). The voltammetric wave shape in this and related systems is consistent with the presence of two one-electron waves separated by ~0.04 V.[27] Using this potential difference, $K \approx 4$ for the mixed-valence equilibrium in eq 5.

$$[2,2,2] + [3,2,3] \rightleftarrows 2[2,2,3] \quad (5)$$

Intravalence Transfer. The [3,2,3] mixed-valence ions have low-energy absorption bands (Figures 3 and 4). Similar low-energy bands have been assigned to IT transitions in related symmetrical, $[(NH_3)_5Ru(L)Ru(NH_3)_5]^{5+}$ (L = pyr,[3] 4,4'-bpy[28]) and $[(bpy)_2ClRu(pyr)RuCl(bpy)_2]^{3+}$,[13] and unsymmetrical, $[(NH_3)_5Ru^{III}(L)Ru^{II}Cl(bpy)_2]^{4+}$,[6] dimers. Our main interest in this work was in the IT properties of the mixed-valence trimeric ions, in part, because of the possibility of observing two effects, both arising from the presence of more than two metal sites. Partial oxidation of the [2,2,2] ions gives [2,2,3] in an equilibrium mixture with [2,2,2] and [3,2,3] (eq 5). In [2,2,3] there are a pentaammine-localized Ru(III) site and two inequivalent ruthenium(II) sites, one adjacent ($-Ru^{II}(bpy)_2-$) and one remote ($-Ru^{II}(NH_3)_5$).

Given the earlier work on unsymmetrical ruthenium dimers, light-induced electron transfer should occur between adjacent

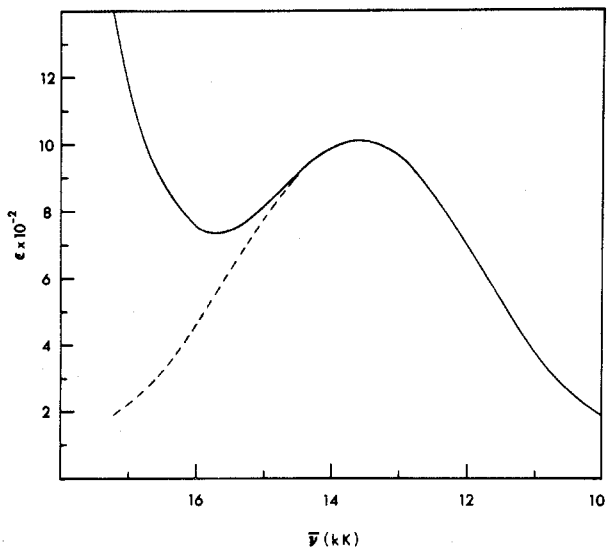

Figure 4. Intervalence transfer band for $[[(NH_3)_5Ru(pyr)]_2Ru(bpy)_2]^{8+}$ in CH_3CN.

Ru(II)–Ru(III) sites (eq 6). The energy of the transition

$$[(NH_3)_5Ru^{III}(L)Ru^{II}(bpy)_2(L)Ru^{II}(NH_3)_5]^{7+} \xrightarrow{h\nu} [(NH_3)_5Ru^{II}(L)Ru^{III}(bpy)_2(L)Ru^{II}(NH_3)_5]^{7+*} \quad (6)$$

should be considerably higher than in a symmetrical case because of the additional equilibrium barrier arising from the unsymmetrical coordination spheres. In addition, long-range intervalence transfer has been reported across 4,4'-bipyridine in the ion $[(NH_3)_5Ru(4,4'\text{-bpy})Ru(NH_3)_5]^{5+}$,[28] in related unsymmetrical ruthenium dimers,[6] and in substituted ferrocenes.[29] If interactions between the terminal ruthenium(II)– and ruthenium(III)–pentaammine groups through the $Ru(bpy)_2(L\text{–})_2^{2+}$ "bridging group" are sufficient, a second IT band should appear, possibly at lower energy (eq 7).

$$[(NH_3)_5Ru^{III}(L)Ru^{II}(bpy)_2(L)Ru^{II}(NH_3)_5]^{7+} \rightarrow [(NH_3)_5Ru^{II}(L)Ru^{II}(bpy)_2(L)Ru^{III}(NH_3)_5]^{7+*} \quad (7)$$

The second special effect which might appear is relevant to the twice-oxidized [3,2,3] ion, where there are two equivalent IT transitions (eq 8 and 9). If delocalization among

$$[3,2,3] \xrightarrow{h\nu} [2,3,3]^* \quad (8)$$

$$[3,2,3] \xrightarrow{h\nu} [3,3,2]^* \quad (9)$$

the Ru sites were extensive, IT excitation would not involve localized Ru(II)–Ru(III) transitions, but rather transitions to delocalized exciton states. In the case of extensive delocalization, distinct IT transitions could occur to the two exciton states, if both are symmetry allowed, giving rise to a splitting in the IT region.

The existence of both effects is tested by the spectrophotometric titration of $[[(NH_3)_5Ru(Pyr)]_2Ru(bpy)_2]^{6+}$ by Br_2 in acetonitrile in Figure 3. In the [3,2,3] ion the band shape appears Gaussian (Figure 4) and only one IT band is observed.[30] The single IT band is consistent with the existence of two weakly interacting or noninteracting IT transitions.

Because of the equilibrium in eq 5, in the initial stages of the titration with Br_2 the ion [2,2,3] is the dominant mixed-valence form in solution. If there were more than one IT transition for [2,2,3], the corresponding IT bands should grow in the initial stages of the titration and decrease as the amount of added Br_2 rises. In fact, an isosbestic point appears in the titration at 710 nm (14.1 kK, Figure 3). The appearance of the isosbestic point, even in solutions where [2,2,2], [2,2,3], and [3,2,3] are all present in significant amounts, shows that the IT properties of the [2,2,3] and [3,2,3] ions are essentially identical. If long-range transfer occurs in the [2,2,3] ion, the intensity of the band is insufficient to observe under the conditions of the experiment.[30] Essentially the same observations were made in an infrared titration of the ion [2,2,2] where L is 4,4'-bipyridine.

The similarity in IT properties between the [2,2,3] and [3,2,3] ions shows that light-induced electron transfer between adjacent $(NH_3)_5Ru^{III}$– and $-Ru^{II}(bpy)_2$– groups is independent of whether the remote pentaammine group is Ru(II) or Ru(III). This argues strongly that remote Ru–Ru interactions between the pentaammine groups are negligible in both [2,2,3] and in [3,2,3], and that the energies of the IT transitions are relatively independent of whether the total charge on the mixed-valence ion is 7+ or 8+. In addition, an exciton model for intervalence transfer in [3,2,3] would appear to be inappropriate. The observed isosbestic point is consistent with the only difference between [2,2,3] and [3,2,3] being the statistical factor of 2 favoring the latter ion where interactions between the two possible transitions are negligible. The appearance of an IT band for the [2,2,3] ion is evidence for the related thermal electron-transfer process,[13] which provides a facile pathway

$$[2,2,3] \rightarrow [2,3,2] \rightarrow [3,2,2]$$

for electron exchange between the pentaammine groups in the [2,2,3] ion.

The assignment of low-energy bands in the mixed-valence ions to IT transitions is supported by two lines of evidence. The first is that bands appear only for the mixed-valence ions (Figure 3). Also, bands do not appear for the [3,2,3] ion where L is BPA. No IT band was observed for the mixed-valence ion $(NH_3)_5Ru^{III}(BPA)Ru^{II}Cl(bpy)_2^{4+}$,[6] and a reasonable conclusion for both systems is that no orbital pathway for metal–metal interaction exists because of the saturated $-CH_2CH_2-$ linkage.

It is possible to estimate the position of $\bar{\nu}_{max}$ for the IT band where L is pyrazine from previous data.[6] For IT transitions involving nonequivalent sites $\bar{\nu}_{max}$ is given by eq 10, where $\bar{\nu}_{FC}$ is the vertical Franck–Condon energy and $\bar{\nu}_0$ is the ground-state internal energy difference following thermal electron transfer (eq 11). $\bar{\nu}_0$ can also be viewed as the energy difference between

$$\bar{\nu}_{max} = \bar{\nu}_{FC} + \bar{\nu}_0 \quad (10)[14]$$

$$[3,2,3] \xrightarrow[\Delta E = \bar{\nu}_0]{} [2,3,3] \quad (11)$$

the valence-state isomers [2,3,3] and [3,2,3], where [2,3,3] is the thermally equilibrated "mixed-valence excited state". $\bar{\nu}_0$ can be estimated as 6.4 kK for the L = pyr ion by using data of Table II and eq 12, if it is assumed that $\Delta S \approx 0$ for

$$\bar{\nu}_0\,(\text{kK}) = 8.07[E_{1/2}' - E_{1/2}(1)] \quad (12)$$

eq 11.[35] In systems where the coordination spheres of the donor and acceptor sites are closely related, e.g., $(NH_3)_5Ru^{III}(pyr)Ru^{II}(bpy)_2(pyr)Ru^{III}(NH_3)_5^{8+}$ and $(NH_3)_5Ru^{III}(pyr)Ru^{II}Cl(bpy)_2^{4+}$, values for $\bar{\nu}_{FC}$ are expected to be similar and the $\bar{\nu}_{max}$ values should be related as in eq 13. For the pyrazine-bridged dimer, $\bar{\nu}_{max}(1) = 10.4$ kK and

$$\bar{\nu}_{max}(2) - \bar{\nu}_{max}(1) = \bar{\nu}_0(2) - \bar{\nu}_0(1) \quad (13)$$

$\bar{\nu}_0(1) \approx 2.4$ kK;[6] using $\bar{\nu}_0(2)$ for [3,2,3] as 6.4 kK gives $\bar{\nu}_{max}(2)$ for [3,2,3] as 14.4 kK. The calculated value is in reasonable agreement with the experimental value (13.7 kK), but slight differences are expected since the potential energy surfaces which determine $\bar{\nu}_{FC}$ should be sensitive to changes in the inner coordination sphere.

The determination of band shapes for the [3,2,3] ions where L is BPE or 4,4'-bpy is difficult without resort to curve-fitting procedures because the IT bands appear as shoulders on intense

MLCT bands. For the L = pyr ion (Figure 4), the bandwidth at half-height, $\bar{\nu}_{1/2}$, can be determined by assuming that the band is symmetrical around $\bar{\nu}_{max}$ (Figure 4). $\bar{\nu}_{1/2}$ is defined as the value of $\Delta\nu$ where eq 14 holds; $A_{\bar{\nu}}$ and A_{max} are the

$$A_{\bar{\nu}}\bar{\nu}_{max}/A_{max}\bar{\nu} = {}^1/_2 \qquad (14)^{14}$$

absorbances at $\bar{\nu}$ and $\bar{\nu}_{max}$, respectively. The experimental value ($\bar{\nu}_{1/2}$ = 4.4 kK) and the value calculated using eq 15

$$\bar{\nu}_{max} - \bar{\nu}_0 = \bar{\nu}_{1/2}{}^2/2.31 \qquad (15)^{14}$$

from the Hush treatment at room temperature (4.1 kK) are in good agreement.

The observation of IT bands for the [3,2,3] ions where L = 4,4'-bpy and BPE is significant since it shows that long-range light-induced and thermal electron transfer can occur between Ru(II) and Ru(III) sites. The band energies are considerably higher than for the L = pyr ion, and data from this and previous work[6,31] suggest that in systems where other molecular features are held constant, $\bar{\nu}_{max}$ is dependent upon the distance separating the metal sites.

A solvent dependence of the energies of IT bands has been predicted by Hush. For a symmetrical dimer, $\bar{\nu}_{max}$ can be related to the inner (λ_i) and outer (λ_o) sphere reorganization terms from the Marcus theory of outer-sphere electron transfer[32] as in eq 16[33] where r_1 and r_2 are the molecular radii

$$\bar{\nu}_{max} = \lambda_i + 4RT + e^2\left(\frac{1}{2r_1} + \frac{1}{2r_2} - \frac{1}{d}\right)\left(\frac{1}{n^2} - \frac{1}{D_S}\right) \qquad (16)$$

of the two sites, d is the distance between the metal sites, and n and D_S are the optical and static dielectric constants for the solvent.[34] For unsymmetrical cases, $\bar{\nu}_{max}$ varies with solvent properties as in eq 17.[33] The expected solvent dependences

$$\bar{\nu}_{max} - \bar{\nu}_0 = \lambda_i + 4RT + e^2\left(\frac{1}{2r_1} + \frac{1}{2r_2} - \frac{1}{d}\right)\left(\frac{1}{n^2} - \frac{1}{D_S}\right) \qquad (17)$$

have been found for the ions $(bpy)_2ClRu(pyr)RuCl(bpy)_2^{3+}$[12] and $(NH_3)_5Ru(pyr)RuCl(bpy)_2^{4+}$.[33] Unfortunately, it is not possible to test eq 17 for the trimeric ions. $\bar{\nu}_{max}$ can be obtained in a variety of solvents. However, $\bar{\nu}_0$ is calculated from redox potentials (eq 12), and the [3,3,3] + e^- → [3,2,3] couple is sufficiently oxidizing that it exceeds the background limits of most of the solvents which were reasonable to use.

A measure of ground-state delocalization in mixed-valence complexes (α^2) can be obtained from eq 18,[1,14] where ϵ_{max} is

$$\alpha^2 = \frac{1}{g_2}\frac{(4.2 \times 10^{-4})\epsilon_{max}\bar{\nu}_{1/2}}{\bar{\nu}_{max}r^2} \qquad (18)$$

the molar extinction coefficient at the IT absorptivity maximum, r is the distance separating the metal centers (6.9 Å for L = pyr), and g_2 is the degeneracy of the excited state. For comparisons with related d^6 Ru dimers, g_2 = 2 for the [3,2,3] trimers and α^2 (per Ru(III)–Ru(II) unit) is 1.5×10^{-3}. This value can be compared with $\alpha^2 = 2.6 \times 10^{-3}$ for $(NH_3)_5Ru(pyr)RuCl(bpy)_2^{4+}$.[6]

Part of the greater delocalization in the dimer arises because of the greater redox inequivalency of the coordination spheres ($\bar{\nu}_0$) for the [3,2,3] ion (~0.8 V vs. ~0.3 V). α^2 can be derived from first-order perturbation theory and should vary inversely with the energy difference between ground and mixed-valence excited states where the latter value can be approximated by $\bar{\nu}_{max}$.[10] Since $\bar{\nu}_{max}$ increases directly with $\bar{\nu}_0$ (eq 10), delocalization is expected to be less for the [3,2,3] ion than in the [2,3] dimer where $\bar{\nu}_0$ is far smaller.

For both the dimer and trimer, the relatively small values of α^2 indicate slight delocalization and essentially localized valences.[1,14] This conclusion is in agreement with other properties of the mixed-valence ions.

In the trimeric mixed-valence ions, there are discrete Ru(II) and Ru(III) valence sites and delocalization is small so that the assumptions made in the Hush treatment are met. The good agreement found between the predicted and experimental properties of the IT bands represents, therefore, an important verification of the Hush theory.

The Hush treatment has now been shown to make successful predictions for the properties of IT bands in the ions $[(NH_3)_5Ru(pyr)]_2Ru(bpy)_2^{8+}$, $(NH_3)_5Ru(pyr)RuCl(bpy)_2^{4+}$, and $(bpy)_2ClRu(pyr)RuCl(bpy)_2^{3+}$. In all three of the ions there is good evidence that discrete Ru(II) and Ru(III) valence sites exist and that Ru(II) → Ru(III) delocalization is relatively slight; deviations found in other systems may occur because of extensive delocalization between the metal centers.

Acknowledgment. We thank the Army Research Office–Durham under Grant DA-ARO-O-31-124-73-G-104 and the Materials Research Center of The University of North Carolina under Grant DAHC15 73 G9 with DARPA for support of this research.

Registry No. $[Ru(bpy)_2(pyr)_2](PF_6)_2$, 40827-50-7; $[Ru(bpy)_2(4,4'\text{-bpy})_2](PF_6)_2$, 40537-44-8; $[Ru(bpy)_2(BPE)_2](PF_6)_2$, 58167-47-8; $[Ru(bpy)_2(BPA)_2](PF_6)_2$, 58167-49-0; $[Ru(NH_3)_5(H_2O)](PF_6)_2$, 34843-18-0; $[[Ru(NH_3)_5(pyr)]_2Ru(bpy)_2](PF_6)_6$, 58167-51-4; $[[Ru(NH_3)_5(4,4'\text{-bpy})]_2Ru(bpy)_2](PF_6)_6$, 58167-53-6; $[[Ru(NH_3)_5(BPE)]_2Ru(bpy)_2](PF_6)_6$, 58167-55-8; $[[Ru(NH_3)_5(BPA)]_2Ru(bpy)_2](PF_6)_6$, 58167-57-0; $[[Ru(NH_3)_5(pyr)]_2Ru(bpy)_2](PF_6)_8$, 58229-37-1; $[[Ru(NH_3)_5(4,4'\text{-bpy})]_2Ru(bpy)_2](PF_6)_8$, 58249-24-4; $[[Ru(NH_3)_5(BPE)]_2Ru(bpy)_2](PF_6)_8$, 58282-07-8; $[[Ru(NH_3)_5(BPA)]_2Ru(bpy)_2](PF_6)_8$, 58282-08-9.

References and Notes

(1) M. B. Robin and P. Day, *Adv. Inorg. Chem. Radiochem.*, **10**, 247 (1967).
(2) H. Taube, *Surv. Prog. Chem.*, **6**, 1 (1973).
(3) C. Creutz and H. Taube, *J. Am. Chem. Soc.*, **91**, 3988 (1969); **95**, 1086 (1973).
(4) E. B. Fleischer and D. H. Lavallee, *J. Am. Chem. Soc.*, **94**, 2583, 2599 (1972).
(5) S. A. Adeyemi, J. N. Braddock, G. M. Brown, J. A. Ferguson, F. J. Miller, and T. J. Meyer, *J. Am. Chem. Soc.*, **94**, 300 (1972); S. A. Adeyemi, E. C. Johnson, F. J. Miller, and T. J. Meyer, *Inorg. Chem.*, **12**, 2371 (1973).
(6) (a) R. W. Callahan, G. M. Brown, and T. J. Meyer, *J. Am. Chem. Soc.*, **96**, 7829 (1974); (b) R. W. Callahan, G. M. Brown, and T. J. Meyer, *Inorg. Chem.*, **14**, 1443 (1975).
(7) G. M. Brown, T. J. Meyer, D. O. Cowan, C. LeVanda, F. Kaufman, P. V. Roling, and M. D. Rausch, *Inorg. Chem.*, **14**, 506 (1975).
(8) J. E. Elias and R. S. Drago, *Inorg. Chem.*, **11**, 415 (1972).
(9) C. Creutz, M. L. Good, and S. Chandra, *Inorg. Nucl. Chem. Lett.*, **9**, 171 (1973).
(10) B. Mayoh and P. Day, *J. Am. Chem. Soc.*, **94**, 2885 (1972).
(11) P. Citrin, *J. Am. Chem. Soc.*, **95**, 6472 (1973).
(12) B. Mayoh and P. Day, *J. Am. Chem. Soc.*, **94**, 2885 (1972).
(13) R. W. Callahan and T. J. Meyer, submitted for publication.
(14) N. S. Hush, *Prog. Inorg. Chem.*, **8**, 391 (1967); N. S. Hush, *Electrochim. Acta*, **13** 1005 (1968).
(15) R. W. Callahan, E. C. Johnson, G. M. Brown, and T. J. Meyer, *ACS Symp. Ser.*, **No. 5** (1974).
(16) T. J. Meyer, *Adv. Chem. Ser.*, in press.
(17) J. A. Ferguson, Ph.D. Thesis, The University of North Carolina, Chapel Hill, N.C., 1971.
(18) L. H. Vogt, Jr., J. L. Katz, and S. E. Wiberly, *Inorg. Chem.*, **4**, 1157 (1965).
(19) D. E. Harrison, H. Taube, and E. Weissberger, *Science*, **159**, 320 (1968).
(20) E. C. Johnson, Ph.D. Thesis, The University of North Carolina, Chapel Hill, N.C., 1975.
(21) P. C. Ford, DeF. P. Rudd, R. G. Gaunder, and H. Taube, *J. Am. Chem. Soc.*, **90**, 1187 (1968).
(22) A. M. Zwickel and C. Creutz, *Inorg. Chem.*, **10**, 2395 (1971).
(23) G. M. Bryant, J. E. Fergusson, and H. K. Powell, *Aust. J. Chem.*, **24**, 257 (1971).
(24) Pt electrodes were cleaned by the procedure recommended by R. W. Adams, "Electrochemistry at Solid Electrodes", Marcel Dekker, New York, N.Y., 1969, p 206.
(25) D. M. Bishop and K. J. Laidler, *J. Chem. Phys.*, **42**, 1688 (1965).
(26) J. N. Murrell and K. J. Laidler, *Trans. Faraday Soc.*, **64**, 371 (1968).
(27) G. M. Brown, Ph.D. Thesis, The University of North Carolina, Chapel Hill, N.C., 1974.
(28) G. M. Tom, C. Creutz, and H. Taube, *J. Am. Chem. Soc.*, **96**, 7827 (1974).

(29) C. LeVanda, D. O. Cowan, C. Leitch, and K. Bechgaard, *J. Am. Chem. Soc.*, **96**, 6788 (1974).
(30) Additional IT bands for either partly or fully oxidized solutions were not observed out to 2600 nm in CH_3CN in a 10-cm cell where [2,2,2] was 10^{-2} M initially.
(31) C. LeVanda, D. O. Cowan, C. Leitch, and K. Bechgaard, *J. Am. Chem. Soc.*, **96**, 6788 (1974).
(32) R. A. Marcus and N. Sutin, *Inorg. Chem.*, **14**, 213 (1975), and references therein.
(33) R. W. Callahan, M. J. Powers, T. J. Meyer, and D. J. Salmon, submitted for publication.
(34) R. A. Marcus, *J. Phys. Chem.*, **67**, 853 (1963); R. A. Marcus, *J. Chem. Phys.*, **43**, 679 (1965).
(35) $\bar{\nu}_0$ is the energy difference between the potentials for the two processes [2,2,2] → [2,3,2] and [2,2,2] → [3,2,2]. Since the first potential cannot be measured directly and since the electron delocalization between the ruthenium centers is small, $E_{1/2}'$, the half-wave potential for the central $Ru(bpy)_2L_2^{2+}$ species as a monomeric unit, is used as an approximation.

Contribution from the Department of Chemistry, Florida State University, Tallahassee, Florida 32306

Metal Carbonyl–Phosphorus Trifluoride Systems. XIII. Fluorine Nuclear Magnetic Resonance Studies on $R_fCo(PF_3)_x(CO)_{4-x}$ Compounds (R_f = CF_3, C_2F_5, C_3F_7)[1]

CARL A. UDOVICH, MARTIN A. KREVALIS, and RONALD J. CLARK*[2]

Received June 3, 1975 AIC504234

A fluorine NMR study has been done on the $R_fCo(PF_3)_x(CO)_{4-x}$ species (R_f = CF_3, C_2F_5, C_3F_7, x = 1–4). All of the species are stereochemically nonrigid at room temperature. In many cases, temperatures approaching −100 °C are required to freeze out the motion. However, even this temperature did not always yield the limiting structure. Two types of dynamic processes have been found: one occurring between different isomers and the other between nonequivalent sites in a single isomer. All of the data are most simply explained by assuming a trigonal-bipyramidal structure with an axial perfluoroalkyl group. In the $CF_3Co(PF_3)_x(CO)_{4-x}$ series when x = 1, there are nearly equal proportions of isomers having axial and equatorial PF_3 groups. The equatorial isomer is increasingly favored for x = 2 and 3. For the species $R_fCo(PF_3)(CO)_3$ of the perfluoroethyl and perfluoropropyl species, the isomer with an axial PF_3 group is strongly favored over the equatorial. For the di- and trisubstituted compounds of this latter series, the isomer with all PF_3 ligands equatorial is sufficiently disfavored that it is not seen at all.

Introduction

The stereochemical nonrigidity of five-coordinate compounds, particularly those in their lower oxidation states, seems now to be a ubiquitous aspect of their structural character.[3] In studies on the species $R_fCo(PF_3)_x(CO)_{4-x}$, where R_f = CF_3, C_2F_5, and C_3F_7 and x = 1–4, the nonrigidity has been clearly demonstrated,[4-6] particularly in the case of $CF_3Co(PF_3)(CO)_3$.[4] At the time of publication of the work on the trifluoromethyl compound,[4] our NMR equipment was not adequate to give us enough confidence to publish the data[6] on the species having a greater degree of NMR complexity. We have now reprepared the species and taken new NMR data on modern equipment. The earlier data[4,6] have by and large been reconfirmed and expanded upon and it is the results of this study that we wish to report.

Experimental Section

The compounds were reprepared using essentially the same procedures as before. The species with a lower PF_3 content disproportionate at a moderate rate. Therefore it was necessary to separate them by gas chromatography under the mildest conditions possible. Also, it was found necessary to store the sealed samples at low temperatures for the same reason. The spectra of the disproportionation products are readily recognizable and are generally sufficiently resolved from the spectrum of the main product to be tolerated in small amounts. On the other hand, trace amounts of decomposition yielded paramagnetic impurities which resulted in poor resolution. Vacuum distillation followed by sealing under vacuum resulted in high-quality spectra when the operations were carefully done.

The NMR samples were run as roughly 10% solutions in an approximately equal-volume mixture of $CFCl_3$ and $CFHCl_2$, using a few percent of $CF_3C_6H_5$ as internal lock and reference. Alternatively, $C_2F_4Br_2$ and $CFHCl_2$, with a lock on the upfield half of the fluorine spectrum of the latter, could be used. The fluorine peak of $C_2F_4Br_2$ broadened too much below −80 °C to be used as lock, but it still served as a good solvent. Spectra were run on a Bruker HFX-90 at 84.66 MHz. The temperature-measuring and -controlling thermocouple was placed just below the NMR tube. It was calibrated by a thermocouple immersed in a blank tube and is felt to be accurate to ±2 °C. For reference purposes, $CFCl_3$ is 63.43 ppm downfield of $CF_3C_6H_5$, and the upfield peak of $CFHCl_2$ is 17.68 ppm upfield of $CF_3C_6H_5$. All chemical shifts are reported as positive downfield of $CF_3C_6H_5$.

Results

There are a number of possible isomers for the various compositions of the system $R_fCo(PF_3)_x(CO)_{4-x}$. Five-coordinate compounds can be either trigonal bipyramidal (TBP) or square-based pyramidal (SBP) with these species most commonly being TBP.[7] The various isomers within such a structure are shown in Figure 1. It is generally found that in these TBP structures a ligand or group like CF_3, which would π bond less than CO (or PF_3), will occupy an axial site.[7] This reduces further the number of isomers but leaves two isomers for each mixed carbonyl–trifluorophosphine composition.

The infrared data[5] in the carbonyl stretching region are not always definitive concerning the number of isomers. For the tricarbonyl, if two isomers are present, five bands are expected. For a single isomer, either three or two bands are expected. Three ir ^{12}CO stretching frequencies, however, are clearly distinguished from the various weak ^{13}CO bands. Therefore, if two isomers are present, there must be a high degree of accidental degeneracy among the bands. For the dicarbonyl, where two stretching bands are expected for either isomer, three bands are seen. The third band indicates the presence of two isomers, but again, one band of the four expected bands is not observed. For the monocarbonyl a shoulder on the major band implies a second isomer.

The room-temperature NMR data indicate a single isomer for each member of the series. The fluorine spectra in the PF_3 region for the mono-, di-, and trisubstituted compounds are similar in appearance to species containing one, two, and three equivalent PF_3 groups.[8] Further, the coupling of the phosphorus atoms to either the CF_3 group or the α fluorines of the C_2F_5 and C_3F_7 groups is indicative of equivalent fluorines. The room-temperature data are given in Table I.